Journal of the European Ceramic Society 17 (1997) 1989–1999

PII: S0955-2219(97)00045-9
0955-2219/97/$17.00 + 0.00

Surface Characterization of Nitrides and Oxynitrides of Groups III_A and IV_A

J. A. Odriozola

Departamento de Química Inorgánica e Instituto de Ciencia de Materiales, Universidad de Sevilla-CSIC, PO Box 874, E-41080 Sevilla, Spain

Abstract

The surface characteristics of nitrides and oxynitrides of groups III_A and IV_A are reviewed, paying attention to the information that can be obtained from the combined use of X-ray photoelectron spectroscopy (XPS) and infrared spectroscopy. Discussion focuses particularly on the hydrolysis mechanism of aluminium nitride and the behaviour of the metal–hydrogen bonds present in hydrogenated silico nitride films, and claimed to be present in aluminium nitride films. © *1997 Elsevier Science Limited.*

1 Introduction

Nitrides and oxynitrides of groups III_A and IV_A of the Periodic Table are of enormous interest from the technological point of view. So, much work has been devoted to characterize their surface structure and reactivity.

Boron, aluminium and silicon nitrides and oxynitrides ceramics are normally used in sintered forms. Nitride powders, like all powders, contain surface impurities as a result of their contact with atmospheric air. These impurities may affect the sintering behaviour of such materials, since the behaviour of powder suspensions is largely controlled by the surface chemistry of the solid.

Stability and rheology of fine-powder slurries is controlled by the chemistry of the solid–solution interface. The particle–particle interactions in a suspension are related to the physico-chemical properties of the solid liquid interface which is mainly dominated in aqueous suspensions by electrical surface charge effects. The interfacial electrochemical properties can be significantly affected by the presence of surface impurities or secondary components added to the suspensions. For non-oxide materials, such as nitrides, the presence of oxygen in the surface region drastically modifies the electrical double-layer properties, e.g. electrokinetic measurements show that the isoelectric points of Si_3N_4 decrease linearly with increasing surface oxide thickness.[1] Moreover, in the case of AlN the oxygen content also influences the heat conductivity of the dense material,[2,3] and in silicon oxynitride films the amount of oxygen affects the number of electron traps in the nitrided film used in ultra-large-scale integration devices such as DRAMs (dynamic random access memories).[4]

The oxidation resistance of nitride materials is an important factor in applications at high temperature in oxidizing environments or in the presence of water. Si_3N_4 is thermodynamically unstable in an oxidizing atmosphere at high temperatures and will react with oxygen.[5] The chemical stability of AlN powders is low and in water hydrolysis takes place.[6–9] The phase composition and microstructure of these ceramics change during oxidation, resulting in changes in the mechanical properties of the materials.[10–12]

Hydrogenated silicon nitride films, SiN_X:H, have attracted increased interest with respect to wide applications as gate insulators in thin film transistors (TFTs). It has been reported that an increase in the incorporated H content leads to deteriorating characteristics of the TFTs having nitride passivation layers.[13] On the other hand, the presence of hydrogen in AlN films is known to passivate dangling bonds affecting the electrical properties of the material.[14]

Most of the problems arising from the formation of passive layers can be clearly understood by means of photoelectron and Auger spectroscopies (XPS and AES) and/or infrared spectroscopy (IR). Moreover, methods based on IR may provide easy access to the determination of structural parameters of interest in the synthesis or preparation of structural materials, e.g. the high temperature

nitriding processes normally used in the manufacture of crystalline silicon nitride, Si_3N_4, ceramic yield materials in which the ratio of the α- and β-Si_3N_4 polymorphic, crystalline modifications varies considerably depending on the actual synthetic conditions employed.[15]

More recently the surface properties of these materials have started to be explored and opportunities in catalytic and sensing technologies are now envisaged. Some time ago the basic properties of silicon oxynitride surfaces and their ability to catalise the Knoevenagel condensation in liquid media were reported.[16,17] Similar behaviour has been reported for a new family of aluminium phosphate oxynitride, AlPON.[18–21] Also the surface properties of germanium-based oxynitrides have been shown to be of technological importance as chemical sensors.[22,23]

As stated above, most of the applications or processing characteristics of these materials are determined by the surface properties, and in consequence extensive studies on them have been undertaken. In this communication a non-exhaustive survey of infrared and X-ray photoelectron spectroscopy studies are reviewed with the aim of ilustrating the different capabilities of these techniques. Special attention will be paid to the *in situ* studies of the surface transformation under realistic conditions which in some way may illustrate the dynamic behaviour of the surfaces under study.

2 Photoelectron Spectroscopy — A Few Basics

Photoelectron spectroscopy (XPS) is an important analytical technique for surface and thin film characterization of solid materials. It provides qualitative and quantitative information relating to the outermost atom or molecule layers. The depth of information or the thickness of the analyzed surface layers ranges from 1 to 3 nm. This mainly depends on the kinetic energy of the photoelectrons. Sputter depth profiling is applied if concentration variations within a thick surface layer are of interest. The XPS spectra are commonly initiated by Mg K_α or Al K_α radiation. The resulting photoelectron lines can be correlated with the binding energy of the core level states of the atoms. That energy can respond sensitively to a charge transfer between neighbouring atoms. It provides a direct insight into chemical bonding parameters. XPS is therefore a powerful tool for the identification of chemical compounds and the modification of the electronic structure. A limitation, however, is the overlapping of several bonding states of different compounds.

3 Infrared Spectroscopy — A Few Basics

In general, when incident radiation interacts with a solid surface, both absorption and reflection occur, with the relative proportions dependent upon the optical properties of the material. The transmissivity of a solid specimen of thickness d depends upon both absorption and reflection effects according to the following expression

$$\tau(\nu) = e^{-\alpha(\nu)d}\tau_R(\nu, d)$$

where the first term represents absorption losses, and the second term those due to single and multiple reflection. The problems associated with the estimation of the reflection losses are severe. Moreover, for intense absorbing solids, d may be as little as a few micrometers, thus creating generally insuperable difficulties in the way of transmission work with single crystals, thin films deposited onto strong absorbing supports or strong absorbers. Clearly, for powdered specimens dispersed, usually in KBr, the experiment is essentially that of determining the transmission spectrum, although even in this case reflectance and particle size effects can cause major disturbances.

The transmission IR spectra of an aluminium-phosphate oynitride sample (AlPON) self-supported pellet become opaque to IR light below 1000 cm^{-1}; the absorption intensity is so high that the transmissivity drops down to zero. If the transmission spectrum is recorded for KBr diluted samples, it reveals the existence of modifications of the intensity and position of the IR bands in the Al–O, P–O, Al–N and P–N regions. These modifications have to be related to changes on the scattering coefficient of the powdered samples related to the presence of the diluent.[24]

The development of Reflectance Infrared Spectroscopy, due to the availability of the Fourier Transform equipment, has dramatically expanded the variety of samples that can be analyzed by IR. Many biological, natural, inorganic and opaque specimens can now be easily studied by a nondestructive method and in their original form.[25] Reflectance Spectroscopy allowed the study of the interaction of liquid- or gas-phase molecules with the surface of the solids providing information concerning darkened areas of strong absorbers, generally below 1000 cm^{-1}.

The main problem in the study of Reflectance Spectroscopy is the presence of the reststrahl region which leads to the apparison of first derivative-like peaks whose maxima do not coincide with the maxima of the absorption coefficients. This phenomenon comes from the nature of the refraction index, n, that is suddenly modified in the

proximity of the absorption maximum. However, by application of the Fresnel formula for the reflectance, R, at normal incidence:

$$R = \left[\frac{\hat{n}-1}{\hat{n}+1}\right]^2$$

it is possible to establish a formula for the frequency-dependent complex dielectric function

$$\frac{\varepsilon(\omega)}{\varepsilon_\infty} = 1 + \frac{\omega_L^2 - \omega_T^2}{\omega_t^2 - \omega^2 - i\gamma\omega}$$

that is directly related to the refractive index through the expressions

$$\hat{n}(\tilde{\nu}) = n(\tilde{\nu})(1 - i\kappa(\tilde{\nu})) = n(\tilde{\nu}) - ik(\tilde{\nu}) = \sqrt{\hat{\varepsilon}(\tilde{\nu})}$$
$$\hat{\varepsilon} = \varepsilon' - i\varepsilon'' \quad \varepsilon' = n^2 - k^2 \quad \varepsilon'' = 2nk$$

An alternative approach to analysis of reflectance spectra makes use of the Kramers–Krönig relation for determining the dielectric function that is built-in software in most modern Fourier Transform Infrared Spectroscopy (FTIR) equipment. Eremets *et al.*[26] by using this approach found fundamental LO and TO modes of cubic boron nitride at 1310 and 1050 cm^{-1}, respectively.

Figure 1 presents the Specular Reflectance (SR) spectrum of an AlN specimen taken at 85° off normal incidence angle. It can be seen as the first derivative-like peak that after Kramers–Krönig transforming it peaks at 989 cm^{-1}. This transformation, however, presents more difficulties in the case of systems with more than a single Lorentz oscillator since the election of ε_0 and ε_∞ is not so evident.

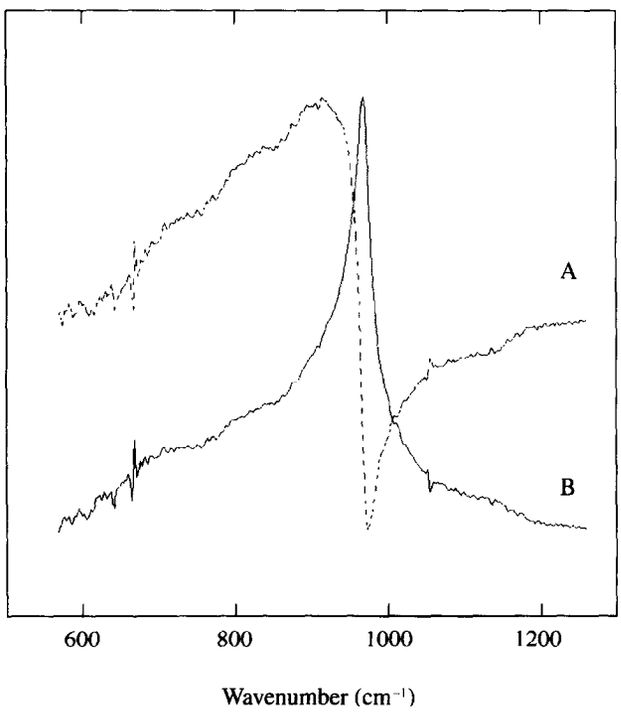

Fig. 1. (A) Specular reflectance spectrum at 85° off normal of AlN powder; (B) Kramers–Krönig transformation of reflectance spectrum.

For the *in situ* study of the reactivity of powdered materials, diffuse reflectance spectroscopy, DRIFT, is becoming a popular technique. In diffuse reflectance the incoming electromagnetic beam undergoes reflection, refraction and absorption processes before reaching the detector. In this way the reflectivity of the sample not only depends upon the refractive index but also upon the absorptivity of the material

$$R = \frac{(\hat{n}-1)^2 + k^2}{(\hat{n}+1)^2 + k^2}$$

where k is the absorption coefficient. At infinite depth, experimentally observed to be of a few mm, and collecting the spectrum over all possible incidence angles, the so-called Kubelka-Munk-Schuster expression holds

$$f(R_\infty) = \frac{k_r}{s} = \frac{1 - R_\infty^2}{2 \cdot R_\infty}$$

where s is the scattering coefficient and R_∞ is the reflectivity at infinite depth. One of the advantages of this experimental procedure is the possibility of relating the reflectance to the concentration of the absorbing species, although, in this case, the reflectance is proportional to the square root of the concentration of the absorbing species.

However, as previously stated, in a conventional experiment both diffuse and specular reflections occur. These are clearly seen in the diffuse reflectance spectrum of AlN samples. A strong absorption is evident at frequencies around 1000 cm^{-1} with a bandshape similar to that found in SR spectroscopy.[7]

Quantitative aspects of DRIFT has been clearly demonstrated. It has been stated that DRIFT spectroscopy may provide information on the apparent activation energy of catalytic reactions by quantifying either the gas-phase products[25] or by analyzing the concentration of adsorbed species.[27] Butler and Huang[28] have successfully applied quantification methods to quantifying the relative proportion of α- and β-Si_3N_4 crystalline polymorphs as a function of the external pressure applied. Both polymorphs crystallize with hexagonal structures in which the basic unit is a tetrahedron. The chief difference between the two modifications is that the β-tetrahedra are slightly more distorted resulting in the presence of characteristic IR bands for both polymorphs, 685, 600, 511, 496 and 460 cm^{-1} for the α-phase and 578 cm^{-1} for the β-phase. The method is based on determining the ratio of the absorbances (I_{685}/I_{578}) of two characteristic marker

bands which appear at 685 cm^{-1} (α-Si_3N_4) and 578 cm (β-Si_3N_4). Table 1 shows the percentage of the α-/β-Si_3N_4 ratio on modifying external pressure.

Rozenberg *et al.*[29] propose a slightly different method for quantifying different phases in pyrolytic boron nitride. The vibrational spectra of h-BN, having tridimensional order, show a band at 817 cm^{-1} that reflects out-of-plane vibrations. The turbostratic modification, t-BN, shows a shift of this band to lower wavenumbers (800 cm^{-1}) and complete absence of tridimensional ordering. Rozenberg *et al.*[29] demonstrate that the shift is mainly determined by the increase in the interlayer distance on going from the hexagonal to the turbostratic structure. This shift allowed identification of five BN structure modifications from IR band shape analysis: hexagonal graphite-like; partially ordered; turbostratic; dense amorphous and highly dispersed amorphous, whose relative content, calculated using calibration samples, can be determined.

The absorption intensity not only depends on the sample concentration but also on the particle size and shape of the samples. Infrared absorption intensity increases with the diminishing of the particle size and reaches constant value with further diminishment. In the examination of DRIFT spectra, if one component has more than two peaks with different intensities, it is expected from theoretical equations that the intensity ratio between those peaks will depend on the particle size of the components. Therefore, the particle size of one component can be determined by using the peak intensity ratio, and the concentration can be determined by comparing the peak intensity to that of a standard material.

In the measurement of diluted samples, the variation of particle size of the sample relates to k_r (the absorption coefficient in reflection) and not to K_t (the absorption coefficient in transmission),[30] according to[15]

$$R = \frac{1 - \frac{2}{(k_1 d)^2}[1 - (1 + k_1 d)e^{-k_1 d}]}{1 - \frac{2}{(k_2 d)^2}[1 - (1 + k_2 d)e^{-k_2 d}]}$$

Since k_1 and k_2 are the intrinsic absorption coefficients of the component, R depends only on d and independently on the concentration of the component. Therefore, the particle size of the component can be determined by measuring R, even if its concentration is unknown. Tsuge *et al.*[15] applied this method to assess the average particle size of α-Si_3N_4 samples from different manufacturers. As reported by Tsuge *et al.*[15] and Butler and Huang[28] powdered α-Si_3N_4 specimens present relatively intense bands at 685–690 and 500 cm^{-1} whose absorption coefficients, k_1 and k_2, can be measured from the intensity of such bands. The comparison of the obtained values for the particle size as a function of the ones measured using a particle size analyzer are shown in Table 2 and the percentage of the α-phase in Table 3. A good correlation exists, except for two samples. The authors[15] suggest that they are in the measured range of particle sizes and that the whole particle size range correponds to the α- and β-phases. However, by close inspection of the relative proportion of α- and β-Si_3N_4 phases it can be observed that the samples with a greater deviation from linearity present percentages of the α-Si_3N_4 phase higher than 75%.

The quantitative power of DRIFT has also been applied to the study of water corrosion of AlN. Highfield and Bowen[8] have shown that after mixing commercial powdered AlN samples with deionized water at room temperature, the area of the OH stretching bands between 3800 and 2400 cm^{-1} follows a linear trend with time, indicating that the hydrolysis degree increases continuously with time as a result of the reaction

$$AlN + 2H_2O \rightarrow AlO(OH) + NH_3$$

By choosing the Al-N stretching overtone at 1330 cm^{-1} these authors confirm the utility of

Table 1. Variation of the α-/β-Si_3N_4 ratio with increasing pressure[28]

Pressure (kbar)	I_{685}/I_{578}	*wt % α-Si_3N_4*
1 atm.	2·63	86
3·1	1·41	76
17·2	1·02	71
18·4	0·98	69

Table 2. Analytical results of particle size (μm) of commercial silicon nitride powders

DRIFT method		*Particle size analyzer*	
Mean	*Std. dev.*	*Mean*	*Range*
1·4	0·3	1·7	3·5–0·5
2·8	0·2	2·3	5·1–0·5
2·9	0·1	1·9	4·0–0·5
1·1	0·1	1·3	2·7–0·4
1·1	0·1	1·1	2·8–0·4
3·0	0·2	1·9	3·7–0·5
1·2	0·2	1·4	2·0–0·4

Table 3. Analytical results of concentration of the α component of commercial silicon nitride powders

DRIFT method		*XRD analysis*
Mean	*Std. dev.*	
22·7	1·2	22·8
68·2	2·1	67·9
73·7	2·2	74·7
74·5	2·9	71·9
83·5	2·2	83·3
89·2	4·9	86·4
92·3	3·0	94·2

DRIFT as a quantitative tool founding a linear correlation between the area of this later band and the amount of AlN present after the hydrolysis treatment.

Furthermore, the capability of controlling the temperature, the pressure and the composition of the reacting atmosphere has converted this technique into a very useful tool in surface chemistry analysis.[31–33] Nowadays the number of DRIFT studies devoted to sample characterization, catalysis and corrosion, for instance, is considerable. It has been reported that the sensitivity advantage for the detection of a surface-deposited species is roughly 4 times that for the same amount distributed evenly through the bulk.[8] This has been interpreted in terms of an effective multipassing of the exciting light due to external, and possibly internal, reflection phenomena. The corollary of this picture is that the core material may become progressively 'hidden' due to specular reflection at the solid–solid interface.

The possibility of studying other sample properties in parallel and simultaneously with the IR analysis is a very interesting aspect that has been recently applied for studying chemical sensor prototypes[22,23] and catalytical properties.[20,21,34]

4 The Combined Use of IR and XPS for Approaching the Structure of Surface Layers

The fundamental Al-N modes have been studied, both theoretically and experimentally. Miwa and Fukumoto[35] performed first-principles pseudopotential calculations on GaN and AlN in the wurzite and zinc-blende structures. In their calculations they found for the optical phonon frequencies active modes, $A_1(TO)$ and $E_1(TO)$, values of 601 and 667 cm^{-1}, respectively. By using the Lyddane–Sachs–Teller relation ($\varepsilon_0 = \varepsilon_\infty \omega_1^2/\omega_t^2$), $\varepsilon_0 = 8{\cdot}50$ and $\varepsilon_\infty = 4{\cdot}68$, it is possible to deduce the frequencies of the LO modes at 810 and 899 cm^{-1}. More recently, Ruiz *et al.*[36] using periodical Hartree–Fock calculations reported a slightly different value, as shown in Table 4.

McMillan *et al.*[37] measured the room temperature reflectance spectra at near normal incidence of thin AlN films deposited by metalorganic chemical vapor deposition. Their results show two absorptions at 650 and 894·5 cm^{-1} in good agreement with the calculations of Miwa and Fukumoto.[35] Mazur,[38] studying AlN films of different thicknesses, by sputtering an aluminium target in the presence of H_2–N_2 mixtures, found a set of bands whose frequencies and ascriptions are presented in Table 5.

Table 4. Active infrared modes of AlN[36]

Mode	*Frequency (cm^{-1})*
$A_1(TO)$	668
$A_1(LO)$	899
$E_1(TO)$	734
$E_1(LO)$	989

However, when the powdered samples are analyzed using diffuse reflectance instead of specular reflectance a down-shift of 115 cm^{-1} is reported. To explain such a shift it is argued that DRIFT spectroscopy provides transmission-like spectra of powders and rough samples while with the specular reflectance method the sensitivity depends on the polarization of the incident radiation with selective excitation of vibrations with dipole transition perpendicular to the film surface.

Benitez *et al.*[7] in a DRIFT study of AlN powdered samples found a band derivative-like at around 1000 cm^{-1}, being the position of the band independent of the preparation method of the AlN samples. In this case, the peak shape indicates the existence of specular reflectance effects that may alter the peak position.

The apparent discrepancies between all of these studies may arise from the nature of the surface layers formed as a result of the hydrolysis undergone by the materials. So, Highfield and Bowen[8] proposed the formation of a bayerite, $Al(OH)_3$, layer on top of an AlN core as a result of the hydrolysis process and Benitez *et al.*[7] found the presence of a surface layer with a very high oxygen content. The formation of coating layers seems to be the most adequate explanation since Ansart and Bernard,[39] in a theoretical and experimental study of AlON materials, found a displacement to lower wavenumbers by increasing the number of oxygen atoms in the co-ordination polyhedra of aluminium.

On the other hand, the study by Loretz *et al.*[14] of

Table 5. Specular reflectance data for 20 nm-thick AlN films[38]

Frequency (cm^{-1})	*Assignments*
660 sh	(TO) AlN
840 s	δ or ν(Al–N_2)
910 s	(LO) AlN
950 s	δ or ν(Al–N_2)
1288 w	AlN combination band
1304 m	δ(NH) in NH_3 co-ordinated to Al
1385 m	δ(NH) in NH_4^+ or ν(NH) in Al–NH^+
1446 w	AlN combination band
1520 m	δ(NH) in NH_3 co-ordinated to Al
1590	δ(NH) in NH_3 co-ordinated to Al
1612 m	δ(NH) in NH_3 co-ordinated to Al
1831–1836 vw	ν(Al–H)
2141–2145 m/w	ν(AlNN)
2900 sh	ν(O–H···N) in $NH_3{\cdot}H_2O$
3220 vw	ν(NH) in NH_3 co-ordinated to Al
3230 m	ν(NH) in NH_3 co-ordinated to Al, NH_4^+, or $NH_3{\cdot}H_2O$
3255 m	ν(NH) in NH_3 co-ordinated to Al, NH_4^+, or $NH_3{\cdot}H_2O$

hydrogenated aluminium nitride films was obtained by radio frequency (r.f.) reactive sputtering of aluminium in the presence of ammonia by means of specular reflectance. They observed a shift of the LO mode of AlN of 115 cm^{-1} on going from 16 (821 cm^{-1}) to 80° (938 cm^{-1}) off normal incidence, whereas the TO mode remains unshifted. At the same time the amplitude of the TO mode decreases continuously on approaching normal incidence conditions. It has been shown that the extent of LO–TO splitting in glass was due to the degree of ionicity of the materials. On this basis Loretz *et al.*[14] suggested that the variation of the LO–TO splitting with the oblique incidence angle could be due to a greater crystal size along the longitudinal excitation when the oblique incidence varies from normal to grazing incidence.

One of the powers of infrared spectroscopy is the characterization of adsorbed species and/or the nature of degraded surface layers after interaction with reactive species.

Air-stabilized AlN powders or thin films present a series of bands ascribed to OH and NH stretchings as a result of the hydrolysis of the surface layers,[7,8,14,20,21,38,40–46] as well as an increase of the surface oxygen concentration as measured by XPS.[7,44–47] By reacting powdered AlN samples with water, Highfield *et al.*[8] observed sharp features at 3656, 3548 and 3440 cm^{-1} that can be seen in the OH stretching region and a new peak at 980 cm^{-1} they assign to bayerite, $Al(OH)_3$. Mazur,[38] in the case of AlN films prepared by ion beam deposition, found that ageing in air does not affect either the intensity or the position of AlN fundamental modes but results in the generation of a new band at 3217 cm^{-1} attributed to NH stretching as a consequence of the hydrolysis of AlN films. Mazur[38] states that this band is due to NH_3 molecules present on the nitride surface coordinated to Al cations. The lack of observation of $\delta(NH_3)$ modes in these experiments is ascribed to the low intensity of these modes that are hidden by strong combination bands of the fundamental AlN modes. However, in the case of hydrogenated AlN films, Wang *et al.*[40] found the presence of a band at 1670 cm^{-1} they ascribed to NH_4OH species adsorbed onto the film surface. Loretz *et al.*[14] fail to observe the band at 1670 cm^{-1} in hydrogenated AlN films and the same result is obtained by Benitez *et al.*[7] and Merle *et al.*[42] for powdered AlN samples. Metselaar *et al.*,[44] characterizing by DRIFT chemically treated AlN powders, observed a band at around 1600 cm^{-1} that they assign to water adsorption.

The presence of NH_4OH would be enhanced by a rapid reaction of NH_3 with atmospheric water. Mazur and co-workers[38,40] suggest that hydrogenated aluminium nitride films with a high concentration of NH_3 are rapidly and also extensively damaged because of high pH values. The presence of a strong NH band at around 3250,[14] 3202,[7] 3217,[38] 3212[42,43] or 3250[41] cm^{-1} and NH peaks[7,14,38,40–43] between 1400 and 1600 cm^{-1} suggest the presence of $R\text{-}NH_2 + OH^-$ or $RR'NH_2 + OH^-$ produced by a rapid hydrolysis of NH sites with atmospheric water. The presence of the OH^- anion would favour the formation of aluminium oxides and/or hydroxydes.

The XPS spectra of AlN powders are characterized by the presence of aluminium, nitrogen and oxygen peaks, indicating in every case the existence of surface hydrolysis as stated by IR measurements. In a careful study of AlN films grown *in situ* over GaAs(100) substrates, Baier and Mönch[48] reported binding energies of 74·3 for Al(2p) and 397·2 eV for N(1s) levels. The binding energy shift of the Al(2p) core level with respect to aluminium metal (72·8 eV) agrees fairly well with charge transfer calculations. In the case of AlN powders binding energy values are reported in Table 6.

The apparent discrepancies observed in the Metselaar *et al.*[44] results have to be ascribed to charging effects that shift the energy scale by around 3 eV.

Liao *et al.*[47] show that the energy difference between Al(2p) lines in AlN and Al_2O_3 is small enough to prevent an accurate deconvolution or ascription of the binding energy value to any defined phase. However, they deconvoluted the X-ray excited Al(2p) peak with two components peaking at around 73·2 and 74·2 eV, the latter being much less intense than the former. Al(2p) binding enregies for γ-Al_2O_3 have been reported at 74·0 by Benitez *et al.*[7] and 73·7 eV by Liao *et al.*,[47] this binding energy being hardly different from that found in AlO(OH) and $Al(OH)_3$.[47]

Bremsstrahlung-excited Al(KLL) lines let Liao *et al.*[47] differentiate between AlN and aluminium oxides and hydroxides leading these authors to postulate the presence of $Al(OH)_3$ surface phases.

The presence of oxygen-rich phases on the surface of air-stabilized or water-treated AlN samples is evident from the quantitations of XPS data. Al/(N + O) ratios fall in the range 0·66 to 0·75 and Al/O ratios are close to 1·0 for air-stabilized samples.[7,14] However, the presence of the aluminium

Table 6. Binding energies of relevant levels of AlN

Ref.	*47*	*7*	*44*	*45*
Al(2p)	*	73·3	76·7–77·4	73·95
N(1s)	396·4	396·4	400·0–400·3	395·9
O(1s)	531·2	530·9	534·7–535·6	530·8
C(1s)	284·6	284·6	287·1–287·8	284·6

hydroxyde is not so evident from the analysis of the DRIFT data.[7] Air-stabilized AlN samples show the same binding energies and surface composition independent of the preparation method. If AlN is obtained by reacting N_2 with aluminium powder mixed with 1·5% wet weight (w/w) $CaCO_3$ at 900°C for 1 h, a calcium carbonate-coated AlN material is obtained. In this case, the surface composition and binding energies remain unaltered with respect to the uncoated samples, but there is no evidence for the presence of hydroxyl groups on their surface. So, an alternative approach to the formation of a bayerite- or boehmite-like outer layer could be the formation of an AlON-like phase. The formation of such a phase would result in the presence of octahedral and tetrahedral aluminium cations which in turn would lead to a Madelung potential on the aluminium cation similar to that found in spinel-like aluminium oxides or hydroxydes. In this way, the binding energy reported by Merle *et al.*[42] for N(1s) holds with this model.

The use of Bremsstrahlung-excited lines has also been successfully studied for silicon nitride and oxynitride ceramics. Okada *et al.*[49] use this approach for characterizing surface-oxidized phases of silicon nitride and silicon oxynitride ceramics due to better separation between energy lines corresponding to different co-ordination polyhedra of silicon changing the O/N ratio. The crystal structure of the oxynitride is composed of SiN_3O tetrahedra having the kinetic energy of the photoelectrons of 1611 eV, around 1 eV less than that of SiN_4 polyhedra present in silicon nitride. Values of 1608 and 1616·5 eV were found for SiO_2 materials and silicon, respectively. It has been shown[1] that for silicon nitride samples having N/Si ratios ranging from 0·92 to 1·19 and O/Si ratios ranging from 0·21 to 0·96 the Si(2p) binding energy is modified from 101·9 to 102·2 eV, demonstrating that the use of Bremsstrahlung-excited Si(KLL) lines provides an easier identification of the different components present in the reacted surface of nitride materials. This technique may also provide a way of estimating the thickness of the oxidic surface layer through the expression[50]

$$t = -2 \cdot 04 \, ln \frac{R}{(R + 1 \cdot 71)}$$

where R is the ratio of the Si_3N_4 and SiO_2 Si(KLL) intensities.

An alternative approach for distinguishing between oxide and nitride groups on the surface has been proposed by Dang and Gnanasekaran,[51] the surface silanol groups present in air-aged Si_3N_4 samples are determined by reaction of the OH groups with tridecafluoro-1,1,2,2-tetrahydrooctyl-1-1-tricholorosilane and further analysis of the F signal.

As stated above, the presence of oxygen within the surface layers of silicon nitride present in microelectronic devices affects the number of electron trap sites, which makes them undesirable for such devices.[52] Lee *et al.*[4] studied by AES the structure of silicon nitride films after wet oxidation. It was seen that the N/O ratio was close to 2 at the surface even for samples for which no wet oxidation was carried out. They also observed a broad oxygen peak deeper in the film, ascribing this later peak to the existence of a native oxide layer at the silicon/silicon nitride interface. The combined use of XPS or AES spectroscopies with Ar^+ sputtering allowed the study of the in-depth composition of surface layers and/or the thin film/substrate interface. Xu *et al.*[53] states, by AES depth profiling, that nitrogen and oxygen concentration are uniformly distributed along the depth of the deposited silicon oxynitride film and gradually reduce towards the Si–N–O/Si interface. These authors also follows Bremsstrahlung-excited silicon lines for determining the co-ordination polyhedra of silicon, but in this case Si(LMM) lines, are selected. As for the case of Si(KLL) lines a shift towards higher kinetic energies is observed on going from SiO_2 (76·2 eV) to Si_3N_4 (82·9 eV) with intermediate values for silicon oxynitride phases (79·1 eV). Following this procedure it is possible to determine the in-depth composition of most of the elements of the Periodic Table. However, no information can be obtained for hydrogen; for solving this problem other approaches can be undertaken, one of the most elegant procedures being the use of Nuclear Reaction Analysis (NRA). In this technique a resonant nuclear reaction is utilized

$$^1H(^{15}N, \alpha\gamma)^{12}C$$

Denisse *et al.*[54] use this method for analyzing the in-depth composition of wet oxidized silicon nitride films. They found that during oxidation, oxygen is incorporated in the upper part of the oxynitride film. Both nitrogen and hydrogen concentrations have strongly decreased in this region presenting the oxidation layer as a sharp interface with the original unoxidized film.

One of the key problems in the preparation of silicon nitride films is the presence of hydrogen within the film structure. Hasegawa *et al.*[13] studied the behaviour of the SiH band present in films prepared by r.f. glow discharge decomposition of SiH_4–NH_3 mixtures. These authors showed that the SiH signal can be deconvoluted in two components at around 2000 and 2100 cm^{-1}, assigned to isolated SiH bonds with no N nearest neighbour

and to N_n-SiH bonds ($n \geq 1$), respectively. By analyzing the behaviour of the SiH and NH bonds as a function of the N/Si ratio, structural information of the film was obtained. On increasing this ratio the intensity of the 2000 cm^{-1} component decreases, disappearing for N/Si ratios around 0·6; conversely the 2100 cm^{-1} component reaches a maximum in intensity for N/Si ratios around 0·5. Hasegawa *et al.*[13] observed a shift of both components of the SiH peak as a function of N/Si ratio that they claim to be due to film stress. A similar shift from 2060 to 2200 cm^{-1} was observed by Fejfar *et al.*[55] on increasing the NH_3 pressure during film preparation; this shift reflects, according to them, the increasing backbonding of Si by N with higher electronegativity, as a result of the Si–H stretching frequency.

In hydrogenated aluminium nitride films, AlN:H, an infrared band at around 2100 cm^{-1} is generally present. Loretz *et al.*[14] assign a band at 2150 cm^{-1} to the N–N vibration of a Al–N_2 complex instead of the Al–H vibration claimed by other authors.[43] Mazur *et al.*[38,40,41] found a band at 2130 cm^{-1}. They also,[40] through mass spectrometry analysis of the gas phase during film preparation, indicated a correlation between the presence of N_2H^+ species and the peak amplitude around 2130 cm^{-1}. Evidence in this line is also provided by Loretz *et al.*[14] by studying the annealing behaviour of AlN thin films under nitrogen. A slight increase in peak amplitude at the expense of a decrease in peak amplitude of NH peak was interpreted as NH bond breaking resulting in AlN_2 complex formation. Merle-Mejean *et al.*,[43] on the contrary, found a band at 2260 cm^{-1} that moves down to 2160 cm^{-1} on heating under inert atmosphere. These bands were attributed to Al–H bond stretching. However, by reacting the samples with D_2, H–D exchange has to be expected, losing the bands in the range 2300–2000 cm^{-1} and producing new ones in the range 1690–1470 cm^{-1}. These authors fail to observe any exchange in the films vacuum outgassed at 770 K (band at 2160 cm^{-1}) and a slight decrease of the 2260 cm^{-1} band on samples outgassed at 570 K. However, in this latter case, the corresponding Al–D stretching band at around 1660 cm^{-1} is not observed, in which case the amplitude decrease may be due to the interaction of the D_2 molecule with a different surface species. By close inspection of Fig. 4 of their paper,[43] a slight decrease of the 2260 cm^{-1} band is observed as well as a small increase in amplitude around 1575 cm^{-1} that they do not designate but cannot be associated to Al–D bonds. Metselaar *et al.*[44] found a band at 2160 cm^{-1} in powdered AlN samples coming from one of the manufacturers. The specimens showing such a peak contain silicon as an impurity, between 1000 and 2000 ppm. As determined by XPS, at least part of such silicon species are present in the material surface. Although noticing that the frequency is quite high for being ascribed to Al–H bond stretching, in aluminium hydrides stretching bands appear at around 1850 cm^{-1}; Metselaar *et al.*[44] follow the criteria reported by Merle-Mejean *et al.*[43] and assign such a band to Al–H bond stretching. It is worth mentioning that these latter authors used for their ascription the stretching frequency of $Si–H_{13}$, 2000-2100 cm^{-1} in silicon nitride films as a criteria for solving the higher-than-expected stretching frequency. Much more recently, Baraton *et al.*[45] added to their study of Al–H bonds XPS measurements. A main peak at 395·9 eV with a minor component at 398·3 eV is observed that, following literature data,[7,14,44] were ascribed to N^{3-} and NH_x species, respectively. An important argument for rejecting the possibility of AlN_2 species was the absence of XPS lines at 400·8 eV that they attributed to the presence of adsorbed N_2 species. However, Shinn and Tsang[56] reported N(1s) binding energies for α-N_2 states and β-N atomic states at 397·5 and 396 eV, respectively, after adsorbing N_2 onto Cr/W(110) surfaces, where the α-N_2 stands for a nitrogen molecule having both nitrogen atoms co-ordinated to metal atoms. Liu *et al.*[46] studying the surface chemistry of aluminium nitride formed on alumina using trimethylaluminum and ammonia as precursors, definitively ruled out the ascription of the bands in the range 2000–2200 cm^{-1} to Al–H species, postulating the formation of AlN_2 complexes perpendicular to the surface.

5 Surface Reactivity

Baraton *et al.*[57,58] studied the surface reactivity of boron nitride powders, prepared by chemical vapour reaction between BCl_3 and NH_3 in a quartz reactor, against different probe molecules. The spectrum of the air-aged samples is dominated by intense bands at 1407 and 797 cm^{-1} that they relate to the hexagonal form of boron nitride, *h*-BN. The reactivity studies are made over self-supported pellets, so, in the region 1650–1000 and 850–700 cm^{-1} intense absorptions occur that completely darken any band present in these regions. In addition to these bands and other weak ones assigned to overtones and/or combination modes, the presence of bands at 3690, 3435, 3565 and 520 cm^{-1} is observed. The band at 3690 cm^{-1} is assigned to ν(OH) in B–OH surface groups whereas the bands at 3565 and 3435 cm^{-1} are ascribed to B–NH_2 groups. A broad and featureless band at 3225 cm^{-1} is assigned to B_2-NH surface groups. By reacting the air-aged samples with D_2, isotopic H–D exchange occurs

and the expected shifts occur for these latter bands. Their presence demonstrates the existence of a hydrolysis mechanism of B–N–B moieties at the surface that results in the formation of B–OH and $B–NH_x$ species.

An interesting aspect pointed out in this paper is the ability of IR spectroscopy to selectively determine the reactivity of different surface groups. The addition of 1 mbar H_2O on an activated sample caused the ν(OH) and ν(NH/NH_2) to increase as a consequence of the following reactions

$$> B - NB_2 + H_2O \rightarrow > B - OH + H - NB_2$$
$$B_2N - H + H_2O \rightarrow > B - OH + B - NH_2$$

The easy hydrolysis of B-N bonds has already been observed in BN films formed by pyrolysis of borazine. Conversely, other films obtained from borane and ammonia and containing mostly NH_2 are inert toward water. This behaviour is explained by considering that the N atom in B_2–NH is forced to be in a trigonal configuration, not the most stable, so weakening the B–N bonds. Water provides the possibility of breaking the B–N bonds and of creating $B–NH_2$ groups in stable pyramidal geometry.

A new family of basic catalysts, amorphous aluminophosphate oxynitrides (ALPON) with variable nitrogen content, have been synthesized by nitridation of amorphous $AlPO_4$ (ALPO).[18–21,34] Samples are analysed by XPS and diffuse reflectance infrared spectroscopy (DRIFTS). The combined use of XPS and *in situ* DRIFTS indicates that nitrogen is preferentially bonded to phosphorous in the AlPON framework. Residual surface NH_4^+ ions coming from the nitridation reaction were used to evaluate the Bronsted acidity of these new catalysts. The decrease in the Bronsted acidity along the series is parallel to a shift of the (P–O) stretching to lower wavenumbers. Malonitrile-benzaldehide condensation is employed as a test reaction to estimate the basicity of (AlPON) samples. The conversion trend observed also correlates with the decrease in the frequency of the (P–O) stretching. Consequently, the position of the (P–O) stretching reflects both the diminishment of the Bronsted acidity and the enhancement of the basicity of the AlPON specimen.

The electrical response of a chemical sensor strongly depends on its composition and the concentration and type of adsorbed species. Infrared spectroscopy is considered as one of the most powerful techniques for the characterization of adsorbed species. Thus, the combination of the analytical resolution of IR with the capabilities of DRIFTS (sample versatility, temperature, pressure and atmosphere control) and the possibility for simultaneous monitoring of electrical properties gives this technique a very high potential for chemical sensor testing. Benitez *et al.*[22] describe a home-made DRIFTS chamber that allows the simultaneous observation of both the electrical response and the DRIFTS spectrum of a cadmium–germanium oxynitride (CdGeON) sensor. Experiments on a CdGeON sensor show some results about its reversible/irreversible behaviour versus temperature and under N_2 atmosphere. A direct relationship between the conductivity and the elimination of DRIFTS peaks at 810, 780 and 580 cm^{-1} is observed. From both DRIFTS spectra and conductivity measurements an explanation involving the presence and filling of vacancies in the solid framework is proposed.[23]

Acknowledgements

Financial support was provided by the European Union under a COST program (D5/06/93) and by Comisión Interministerial de Ciencia y Tecnología (MAT94-0434-C03-02).

References

1. Bergström, L. and Bostedt, E., Surface chemistry of silicon nitride powders: electrokinetic behaviour and ESCA studies. *Coll. Surfaces*, 1990, **49**, 183–197.
2. Kasori, M., Ueno, F. and Tsuge, A., Effects of transition-metal additions on the properties of AlN. *Journal of the American Ceramic Society*, 1994, **77**, 1991–2000.
3. Hirano, M. and Yamauchi, N., Development of as-fired aluminium nitride substrates with smooth surface and high thermal conductivity. *Journal Mater. Sci.*, 1993, **28**, 5737–5743.
4. Lee, E. G., Im, H. B. and Roh, J. S., Effects of wet oxidation on the properties of sub-10nm-thick silicon nitride films. *Journal of the American Ceramic Society*, 1991, **74**, 1563–1568.
5. Habraken, F.H.P.M. and Kuiper, A. E. T., Silicon nitride and oxynitride films. *Mater. Sci. Eng. R*, 1994, **12**, 123–175.
6. Egashira, M., Shimizu, Y., Takao, Y., Yamaguchi, R. and Ishikawa, Y., Effect of carboxylic acid adsorption on the hydrolysis and sintered properties of aluminum nitride powder. *Journal of the American Ceramic Society*, 1994, **77**, 1793–1798.
7. Benítez, J. J., Centeno, M. A., Capitán, M. J., Odriozola, J. A., Viot, B., Verdier, P. and Laurent, Y., Study of corrosion-protected AlN samples by x-ray photoelectron spectroscopy and diffuse reflectance IR Fourier transform spectroscopy. *Journal Mater. Chem.*, 1995, **5**, 1223–1226.
8. Highfield, J. G. and Bowen, P., Diffuse-reflectance Fourier transform infrared spectroscopic studies of the stability of aluminum nitride powder in an aqueous environment. *Anal. Chem.*, 1989, **61**, 2399–2402.
9. Egashira, M., Shimizu, Y. and Takatsuki, S., Chemical surface treatments of aluminium nitride powder suppressing its reactivity with water. *Journal Mater. Sci.*, 1991, **10**, 994–996.
10. Jansen, F., Day, A. and Wamboldt, L., On the chemical and mechanical properties of sputtered silicon nitride films. *Thin Solid Films*, 1992, **19**, 139–145.

11. Natansohn, S., Pasto, A. E. and Rourke, W. J., Effect of powder surface modifications on the properties of silicon nitride ceramics. *Journal of the American Ceramic Society*, 1993, **76**, 2273–2284.
12. Ohashi, M., Kanzaki, S. and Tabata, H., Processing, mechanical properties, and oxidation behaviour of silicon oxynitride ceramics. *Journal of the American Ceramic Society*, 1991, **74**, 109–114.
13. Hasegawa, S., Amano, Y., Inokuma, T. and Kurata, Y., Relationship between the stress and bonding properties of amorphous SiN_x:H films. *Journal Appl. Phys.*, 1992, **72**, 5676–5681.
14. Loretz, J. C., Despax, B., Marti, P. and Mazel, A., Hydrogenated aluminum nitride thin films prepared by r.f. reactive sputtering. Infrared and structural properties. *Thin Solid Films*, 1995, **265**, 15–21.
15. Tsuge, A., Uwamino, Y., Ishizuka, T. and Suzuki, K., Quantitative analysis of powdery sample by diffuse reflectance infrared Fourier transform spectrometry: determination of the α-component in silicon nitride. *Appl. Spectrosc.*, 1991, **45**, 1377–1380.
16. Lednor, P.W. and de Ruiter, R. The use of high surface area silicon oxynitride as a solid, basic catalyst. *Journal Chem. Soc. Chem. Commun.*, 1991, pp. 1625–1626.
17. Lednor, P. W., Synthesis, stability, and catalytic properties of high surface area silicon oxynitride and silicon carbide. *Catal. Today*, 1992, **15**, 243–261.
18. Gandía, L. M., Malm, R., Marchand, R., Conanec, R., Laurent, Y. and Montes, M., Application of a new hydrogenated aluminophosphate oxynitride (AlPON) as a catalytic support for the one-step synthesis of methyl isobutyl ketone from acetone. *Appl. Catal. A*, 1994, **114**, L1–L7.
19. Grange, P., Bastians, Ph., Conanec, R., Marchand, R. and Laurent, Y., Influence of nitrogen content of a new aluminophosphate oxynitride catalyst: AlPON in Knoevenagel condensation. *Appl. Catal. A*, 1994, **114**, L191–L196.
20. Grange, P., Bastians, Ph., Conanec, R., Marchand, R., Laurent, Y., Gandía, L., Montes, M., Fernández, J. and Odriozola, J. A., A new strong basic high surface area catalyst. The nitrided aluminophosphate: AlPON and Ni-AlPON. *Stud. Sur Sci. Catal.*, 1995, **91**, 381–389.
21. Benítez, J. J., Odriozola, J. A., Marchand, R., Laurent, Y. and Grange, P., Surface basicity of a new family of catalysts: aluminophosphate oxynitride (AlPON). *Journal Chem. Soc. Faraday Trans.*, 1995, **91**, 4477–4479.
22. Benítez, J. J., Centeno, M. A., Merdrignac, O. M., Guyader, J., Laurent, Y. and Odriozola, J. A., DRIFTS chamber for *in situ* and simultaneous study of infrared and electrical response of sensors. *Appl. Spectrosc.*, 1995, **49**, 1094–1096.
23. Benítez, J. J., Centeno, M. A., Louis dit Picard, C., Guyader, J., Laurent, Y. and Odriozola, J. A., Influence of oxygen in the sensing properties of cadmium and germanium oxynitride. *Langmuir*, 1996, **12**, 1495–1499.
24. Benítez, J. J. and Odriozola, J. A., Unpublished data.
25. Benítez, J. J., Carrizosa, I. and Odriozola, J. A., Simultaneous analysis of gas phase and intermediates in the hydrogenation of carbon oxides by DRIFTS. *Appl. Spectrosc.*, 1993, **47**, 1760–1766.
26. Eremets, M. I., Gauthier, M., Polian, A., Chervin, J. C. and Besson, J. M., Optical properties of cubic boron nitride. *Phys. Rev. B*, 1995, **52**, 8854–8863.
27. Benítez, J. J., Carrizosa, I. and Odriozola, J. A., HCOOH hydrogenation over lanthanide-oxide-promoted Rh/Al_2O_3 catalysts. *Appl. Sur Sci.*, 1993, **68**, 565–573.
28. Butler, I. S. and Huang, Y., Infrared study of the effect of high external pressures on crystalline α-silicon nitride. *Appl. Spectrosc.*, 1992, **46**, 1303–1304.
29. Rozenberg, A. S., Sinenko, Y. A. and Chukanov, N. V., Ir spectroscopy characterization of various types of structural irregularities in pyrolytic boron nitride. *Journal Mater. Sci*, 1993, **28**, 5675–5678.
30. Adams, D. M., Vibrational spectroscopy, in A. K. Cheetham and P. Day ed., *Solid State Chemistry: Techniques*, Oxford University Press, Oxford, 1987.
31. Benítez, J. J., Alvero, R., Capitan, M. J., Carrizosa, I. and Odriozola, J. A., DRIFTS study of adsorbed formate species in the carbon dioxide and hydrogen reaction over rhodium catalysts. *Appl. Catal.*, 1991, **71**, 219–231.
32. Benítez, J. J., Alvero, R., Carrizosa, I. and Odriozola, J.A., 'In situ' DRIFTS study of adsorbed species in the hydrogenation of carbon oxides. *Catal. Today*, 1991, **9**, 53–60.
33. Malet, P., Benítez, J. J., Capitan, M. J., Centeno, M. A., Carrizosa, I. and Odriozola, J. A., EXAFS and DRIFTS study of lanthanide doped rhodium catalysts. *Catal. Lett.*, 1993, **18**, 81–97.
34. Benítez, J. J., Díaz, A., Laurent, Y., Grange, P. and Odriozola, J. A., Diffuse reflectance infrared (DRIFTS) and mass spectrometry study of thermal stability of aluminophosphate oxynitrides (AlPON). *Z. Phys. Chem.*, (submitted).
35. Miwa, K. and Fukumoto, A., First-principles calculation of the structural, electronic, and vibrational properties of gallium nitride and aluminum nitride. *Phys. Rev. B*, 1993, **48**, 7897–7902.
36. Ruiz, E., Alvarez, S and Alemany, P., Electronic structure and properties of AlN. *Phys. rev. B*, 1994, **49**, 7115–7123.
37. MacMillan, M. F., Devaty, R. P. and Choyke, W. J., Infrared reflectance of thin aluminum nitride films on various substrates. *Appl. Phys. Lett.*, 1993, **62**, 750–752.
38. Mazur, U., Infrared study of AlN films prepared by ion beam deposition. 1. Effects of film thickness, aging, and moisture. *Langmuir*, 1990, **6**, 1331–1337.
39. Ansart, F. and Bernard, J., Infrared optical properties of aluminum oxynitride films. *Phys. Stat. Sol. A*, 1992, **134**, 467–473.
40. Wang, X.-D., Hipps, K. W. and Mazur, U., Infrared and morphological studies of hydrogenated AlN thin films. *Langmuir*, 1992, **8**, 1347–1353.
41. Wang, X.-D., Hipps, K. W. and Mazur, U., Infrared study of ion beam deposited hydrogenated AlN thin films. 2. Effect of deuterium substitution. *Journal Phys. Chem.*, 1992, **96**, 8485–8488.
42. Merle, T., Baraton, M. I., Goeuriot, D., Quintard, P. and Lorenzelli, V., Characterization of nitrided high surface γ-alumina powders. *Journal Mol. Struct.*, 1992, **267**, 341–346.
43. Merle-Méjean, T., Baraton, M. I., Quintard, P., Laurent, Y. and Lorenzelli, V., Fourier-transform infrared characterization of an aluminium nitride surface. *Journal Chem. Soc. Faraday Trans.*, 1993, **89**, 3111–3115.
44. Metselaar, R., Reenis, R., Chen, M., Gorter, H. and Hintzen, H. T., Surface characterization of chemically treated aluminium nitride powders. *Journal of the European Ceramic Society*, 1995, **15**, 1079–1085.
45. Baraton, M.I., Chen, X. and Gonsalves, K.E., FT-IR analysis of the surface of nanostructured aluminum nitride powder prepared via chemical synthesis. *Journal Mater. Chem.* (in press).
46. Liu, H., Bertolet, D. C. and Rogers Jr, J. W., The surface chemistry of aluminum nitride MOCVD on alumina using trimethylaluminum and ammonia as precursors. *Sur Sci.*, 1994, **320**, 145–160.
47. Liao, H. M., Sodhi, R. N. S. and Coyle, T. W., Surface composition of AlN powders studied by x-ray photoelectron spectroscopy and Bremsstrahlung-excited Auger electron spectroscopy. *Journal Vac. Sci. Technol. A*, 1993, **11**, 2681–2686.
48. Baier, H. U. and Mönch, W., Formation of aluminum nitride films on GaAs(110) at room temperature by reactive molecular-beam epitaxy: x-ray and soft x-ray photoemission spectroscopy. *Journal Appl. Phys.*, 1990, **68**, 586–590.
49. Okada, K., Fukuyama, K and Kameshima, Y., Characterization of surface-oxidized phase in silicon nitride and

silicon oxynitride powders by x-ray photoelectron spectroscopy. *Journal of the American Ceramic Society*, 1995, **78**, 2021–2026.
50. Hackley, V. A., Wang, P. S. and Malghan, S. G., Effects of soxhlet extraction on the surface oxide layer of silicon nitride powders. *Mater. Chem. Phys.*, 1993, **36**, 112–118.
51. Dang, T. A. and Gnanasekaran, R., Enhancement of electron spectroscopy for chemical analysis of surface silanol in silicon nitride through chemical derivatization. *Journal Vac. Sci Technol. A*, 1991, **9**, 1406–1409.
52. Hori, T., Iwasaki, H. and Tsuji, T., Electrical and physical properties of ultrathin reoxidized nitrided oxides prepared by rapid thermal processing. *IEEE Trans. Electron Devices*, 1989, **ED-36**, 340–350.
53. Xu, X. L., McLarty, P. K., Brush, H., Misra, V., Wortman, J. J. and Harris, G. S., Characterization of thin silicon oxynitride films prepared by low pressure rapid thermal chemical vapor deposition. *Journal Electrochem. Soc.*, 1993, **140**, 2970–2974.
54. Denisse, C. M. M., Smulders, H. E., Habraken, F. H. P. M. and van der Weg, W. F., Oxidation of plasma enhanced chemical vapour deposited silicon nitride and oxynitride films. *Appl. Sur Sci*, 1989, **39**, 25–32.
55. Fejfar, A., Zemek, J. and Trchová, M., Hydrogen and nitrogen bonding in silicon nitride layers deposited by laser reactive ablation: infrared and x-ray photoelectron study. *Appl. Phys. Lett.*, 1995, **67**, 3269–3271.
56. Shinn, N. D. and Tsang, K. L., Strain-induced surface reactivity: low temperature Cr/W(110) nitridation. *Journal Vac. Sci. Technol. A*, 1991, **9**, 1558–1562.
57. Baraton, M. I., Merle, T., Quintard, P. and Lorenzelli, V., Surface activity of a boron nitride powder: a vibrational study. *Langmuir*, 1993, **9**, 1486–1491.
58. Baraton, M. I., Boulanger, L., Cauchetier, M., Lorenzelli, V., Luce, M., Merle, T., Quintard, P. and Zhou, Y. H., Nanometric boron nitride powders: laser synthesis, characterization and FT-IR surface study. *Journal of the European Ceramics Society*, 1994, **13**, 371–378.